PARTICLE DETECTION:
AN OVERVIEW OF THE STATE OF THE ART

Workshop on Physics and Instrumentation
with 6 - 12 GeV Beams
Jefferson Lab
15 - 18 June 1998

Peter Weilhammer
CERN EP Division

CONTENT OF TALK

The Plethora of detection principles employed in existing collider experiments like at LEP, SLC, HERA and TEVATRON and in future planned experiments at high luminosity colliders, e.g. ATLAS, CMS, LHC-B and ALICE at LHC, CDF and D0 upgrade at the TEVATRON, BABAR and BELLE at SLAC and KEK B-factories, and heavy ion experiments at RHIC present themselves as a guideline for this overview.

The available time only permits a brief discussion of some of the techniques. I will be able to go into a bit more detail in the field of semiconductor position sensitive detectors, which are the only ones I understand to some extent.

Most of the material for this talk I have taken from a set of excellent lectures on Particle Detectors given by Christian Joram in the CERN Academic Training Program given in March 1998 (available on the CERN Website). I would like to thank Christian here for allowing me to tap so extensively into his work.

- **GASEOUS DETECTORS**
  - Multiwire Proportional Chamber MWPC) and Derivations
  - Drift Chambers
  - Micro Gaseous Chambers
- **SEMICONDUCTOR DETECTORS**
  - Silicon Detectors
  - CVD Diamond Detectors
- **SCINTILLATION DETECTORS**
  - Scintillators
  - Scintillating Fibre Trackers

- **PHOTODETECTORS**
  - PMT
  - Micro Channel Plates
  - Visible Light Photo Counters
  - Hybrid Photo Detectors (Diodes)
- **PARTICLE IDENTIFICATION**
  - dE/dx
  - Time of Flight
  - Cerenkov Detectors

Requirements on Position Sensitive Detectors in Particle Physics

- **TRACKING**

in particle physics experiments:

4-vector {p} = [E,p(x),p(y),p(z)]

The MOMENTUM components can be derived from the measurement of the particle trajec-tory in a magnetic field.

Requirements on position resolution are particu-larly high for high-energy collider experiments since lever arms cannot be made large.

σ_x from several μm to a few hundred μm

Both gaseous and semiconductor detectors

- **VERTEXING**

Separation of secondary from primary vertices.

Example: B-decays, τ-decays

Precision of better than 10 μm desirable for impact parameter resolution of around 20 mm

So far semiconductor sensors have been employed in experiments at the SPS, LEP, SLC, Fermilab, Cornell, Frascati, …and will be employed on a big scale in future Collider experiments

v **PARTICLE IDENTIFICATION**

For RICH detectors positive measurement in the mm range is often sufficient. Photo detection for UV/visible light photons from a Cerenkov radiator.

J **CALORIMETRY**

Coarse measurement of position

Best possible energy measurement

Introduction

- **A W^+W^- decay in DELPHI**

e^+e^- ($\sqrt{s}$=161.2 GeV) $\rightarrow W^+W^- \rightarrow q\bar{q}\bar{q}q \rightarrow$ 4 hadronic jets

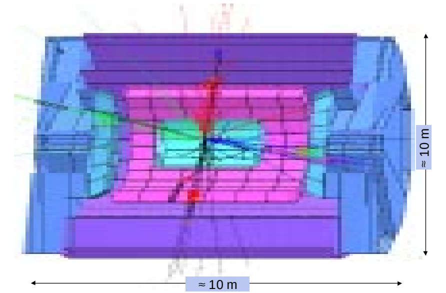

Introduction

- **Reconstructed B-mesons in the DELPHI micro vertex detector**

$\tau_B \approx 1.6$ ps $\quad l = c\tau\gamma \approx 500\ \mu m \cdot \gamma$

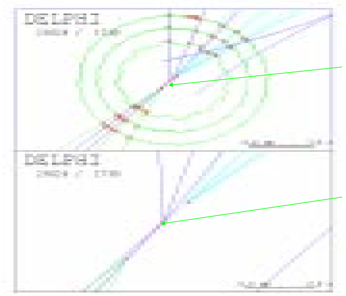

Introduction

Reconstructed high density tracks in the main TPC of NA49

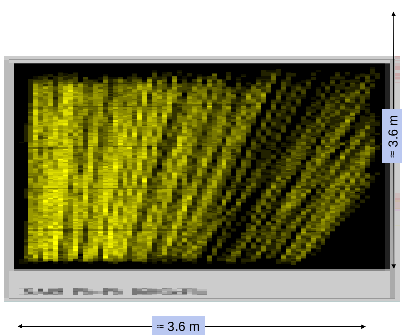

Introduction

- **A simulated event in ATLAS (CMS)**

$H \rightarrow 4\mu$

pp collision at $\sqrt{s}$ = 14 TeV
$\sigma_{inel.} \approx 70$ mb
Interested in processes with $\sigma \approx 10$–100 fb

L = 10^{34} cm^{-2} s^{-1}, bunch spacing 25 ns

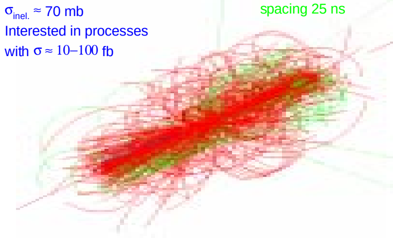

≈ 23 overlapping minimum bias events / BC
≈ 1900 charged + 1600 neutral particles / BC

Multi wire proportional chambers

Multi wire proportional chambers (MWPC)

(G. Charpak et al. 1968, Nobel prize 1992)

Capacitive coupling of non-screened parallel wires? Negative signals on all wires? Compensated by positive signal induction from ion avalanche.

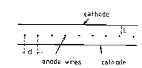

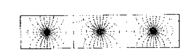

field lines and equipotentials around anode wires

Typical parameters: L=5mm,d=1mm,a_{wire}=20μm.

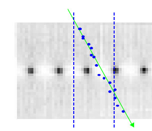

Normally digital readout: spatial resolution limited to

$\sigma_x \approx \sqrt{d}$
(d=1mm, σ_x=300 μm)

Address of fired wire(s) give only 1-dimensional information. Secondary coordinate ….

Multi wire proportional chambers

Secondary coordinate

- Crossed wire planes. Ghost hits. Restricted to low multiplicities. Also stereo planes (crossing under small angle).

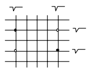

- **Charge division. Resistive wires (Carbon,2kΩ/m).**

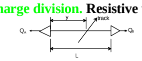

$$\frac{y}{L} = \frac{Q_B}{Q_A + Q_B} \quad \sigma\left(\frac{y}{L}\right) \text{ up to } 0.4\%$$

- **Timing difference (DELPHI Outer detector, OPAL vertex detector)**

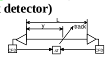

$$\sigma(\Delta T) = 100\,ps$$
$$\rightarrow \sigma(y) \approx 4cm \quad \text{(OPAL)}$$

- **1 wire plane + 2 segmented cathode planes**

  Analog readout of cathode planes.
  $\rightarrow \sigma \approx 100\ \mu m$

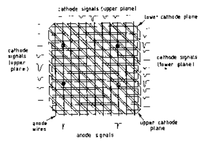

Derivatives of proportional chambers

Some 'derivatives'

- **Multistep avalanche chambers**

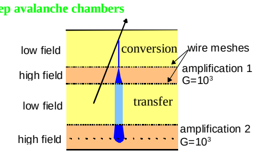

≥ 2 parallel plane avalanche chambers **(PPAC)**, separated by transfer fields, operated at low gain.

Achieve high total gain (10^6-10^8) by reducing feedback photon problem.

Electron transparency of wire meshes depends on field ratio E_{out}/E_{in}. ($E_{out}/E_{in} = 0.1 \rightarrow T \approx 0.1$)

Charge amplification by Penning process at rel. low field:
$A^* + C \rightarrow A + C^+ + e^-$

Application: Single photo electron detection.

Derivatives of proportional chambers

- **Thin gap chambers (TGC)**

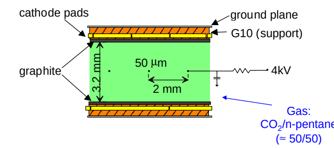

Operation in saturated mode. Signal amplitude limited by by the resistivity of the graphite layer
(≈ 40kΩ/◆).

Fast (2 ns risetime), large signals (gain 10^6), robust

Application: OPAL pole tip hadron calorimeter.
G. Mikenberg, NIM A 265 (1988) 223
ATLAS muon endcap trigger, Y.Arai et al. NIM A 367 (1995) 398

Derivatives of proportional chambers

- **Resistive plate chambers (RPC)**

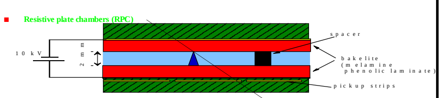

Gas: $C_2F_4H_2$, (C_2F_5H) + few % isobutane
(ATLAS, A. Di Ciaccio, NIM A 384 (1996) 222)

Time dispersion ≈ 1..2 ns → suited as trigger chamber
Rate capability ≈ 1 kHz / cm^2

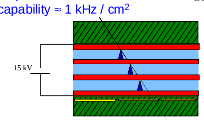

Double and multigap geometries → improve timing and efficiency

Problem: Operation close to streamer mode.

Drift chambers

Drift chambers

(First studies: T. Bressani, G. Charpak, D. Rahm, C. Zupancic, 1969
First operation drift chamber: A.H. Walenta, J. Heintze, B. Schürlein, NIM 92 (1971) 373)

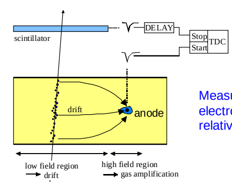

Measure arrival time of electrons at sense wire relative to a time t_0.

What happens during the drift towards the anode wire ?

- Drift velocity (with and without B-fields)
- Diffusion (with and without B-fields)

Drift and diffusion in gases

Drift and diffusion in gases

No external fields: Electrons and ions will lose their energy due to collisions with the gas atoms → thermalization

$$\varepsilon = \frac{3}{2}kT \approx 40\ \text{meV}$$

Undergoing multiple collisions, an originally localized ensemble of charges will diffuse

$$\frac{dN}{N} = \frac{1}{\sqrt{4\pi Dt}} e^{-(x^2/4Dt)}\,dx$$

$$\sigma_x(t) = \sqrt{2Dt} \quad or \quad D = \frac{\sigma_x^2(t)}{2t}$$

D: diffusion coefficient

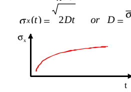

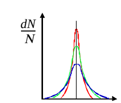

In the presence of electric and magnetic fields the equation of motion is

$$m\frac{d\vec{v}}{dt} = e\vec{E} + e(\vec{v} \times \vec{B}) + \vec{Q}(t)$$

Q(t) represents a stochastic force resulting from the multiple scattering.

Drift chambers

The spatial resolution is not limited by the cell size
→ less wires, less electronics, less support structure than in MWPC.

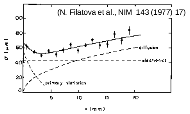

Resolution determined by diffusion, path fluctuations, electronics and primary ionization statistics

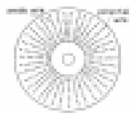

Various geometries of cylindrical drift chambers

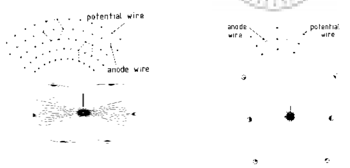

Drift chambers

Straw tubes: Thin cyclindrical cathode, 1 anode wire

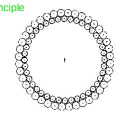

Example: DELPHI Inner detector
5 layers with 192 tubes each
tube ∅ 0.9 cm, 2 m long,
wall thickness 30 μm (Al coated polyester)
wire ∅ 40 μm
Intrinsic resolution ca. 50 μm

Jet chambers: Optimized for maximum number of measurements in radial direction

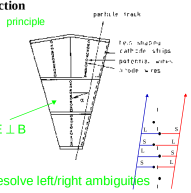

Resolve left/right ambiguities

Example: OPAL Jet chamber
Ø=3.7m, L=4m, 24 sectors à 159 sense wires (±100 μm staggered). 3 cm < l_{drift} < 25 cm

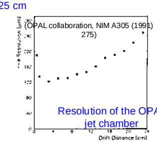

Resolution of the OPAL jet chamber

Drift Chambers

Time Projection Chamber → full 3-D track reconstruction

- **x-y from wires and segmented cathode of MWPC**
- **z from drift time**
- **in addition dE/dx information**

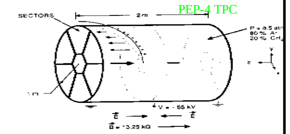

Diffusion significantly reduced by B-field.
Requires precise knowledge of v_D → LASER calibration + p,T corrections

Drift over long distances → very good gas quality required

Space charge problem from positive ions, drifting back to midwall → gating

ALEPH TPC
(ALEPH coll., NIM A 294 (1990) 121, W. Atwood et. Al, NIM A 306 (1991) 446)

Ø 3.6M, L=4.4 m

$\sigma_{R\phi} = 173$ μm
$\sigma_z = 740$ μm
(isolated leptons)

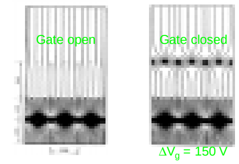

$\Delta V_g = 150$ V

Drift chambers

NA 49: Use of TPC's for high multiplicity tracking in heavy ion collisions.

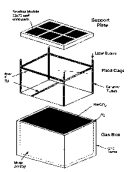

- 2 Vertex + 2 Main TPC's, modular construction.
- In total 50 m³ sensitive volume, 180.000 electronic channels.
- 'Cold' gas mixtures (Ne-CO_2 (90-10), Ar-CO_2-CH_4 (90-5-5) → low diffusion.

(NIM A360 (1995) 52)

Drift chambers

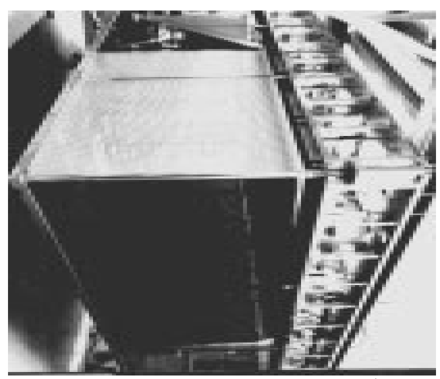

NA 49 Main TPC

Drift chambers

A central Pb-Pb interaction in the main TPC (size ca. 3.6 x 3.6 m²):
Only the projection of a drift time slice (≈ 10 cm) is shown.
500-600 tracks can be reconstructed, resolution ≈ 200μm.

- Very sophisticated track finding algorithms required.

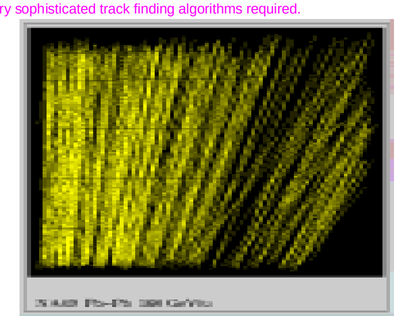

Micro gaseous detectors

Faster and more precision ? → smaller structures

■ **Microstrip gas chambers** (A. Oed, NIM A 263 (1988) 352)

geometry and typical dimensions (CMS standard)

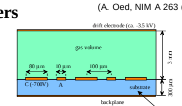

Field geometry

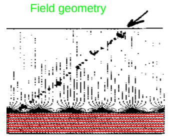

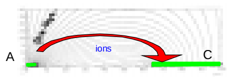

Fast ion evacuation → high rate capability $\approx 10^6$ /(mm^2·s)

Gas: Ar-DME, Ne-DME (1:2), Lorentz angle 14° at 4T.
Gain $\leq 10^4$
Passivation: non-conductive protection of cathode edges
Resolution: ≈ 30..40 μm
Aging: Seems to be under control.
10 years LHC operation ≈ 100 mC/cm

CMS

Micro gaseous detectors

Micro gap chambers

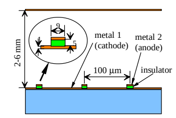

F. Angelini, NIM A 335 (1993) 69

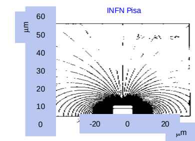

2-dimensional readout with MGC (Bellazini)

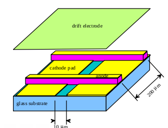

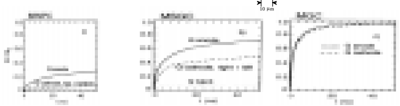

Micro gaseous detectors

■ **Micro Gap Wire Chamber** (E. Christophel et al., NIM A 398 (1997) 195)

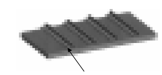

Gain > 10^5 (prototype 2.6 x 2.6 cm^2)

■ **MICROMEGAS** (G. Charpak et al., CERN-LHC/97-08)

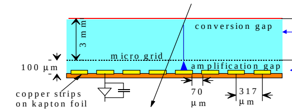

Gas: Ar-DME (≈80:20)
High rate capability (10^9 /(mm^2·s), prototype in test beam

Micro gaseous detectors

υ GEM: The Gas Electron Multiplier

(R. Bouclier et al., NIM A 396 (1997) 50)

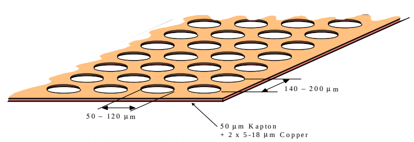

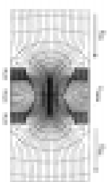

Micro gaseous detectors

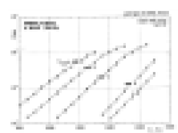

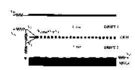

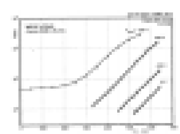

Gas Detector Aging

Detector Aging

Very detailed reviews:
J. Va'vra SLAC-PUB-5207
J. Kadyk A300 (1991) 436

A very complex subject !

Avalanche formation ≈ micro plasma discharge

→ **decomposition of chamber gas + possible contaminants**
→ **highly active radicals with dipole moments**
→ **polymerization**
→ **resistive deposits on anodes and cathodes(Carbon, oxides, silicon compounds)**

anode wires: increase of diameter, electron 'jam' on wire → reduced and inhomogeneous field, rate -dependent gain

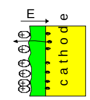

cathodes: formation of strong dipoles from ions and mirror charge → Malter effect, field emission of electrons → dark current

+ **'noisy wires', sparking (sparks can also lead to corrosion and evaporation of electrodes)…**

Aging rate = relative amplitude loss ∝ charge deposition on anode.

Specific aging R [%/(C/cm)]: $\Delta A = R\,Q$

Gas Detector Aging

R can vary from negligible values <10 (Ar/C_2H_6 50/50)
to catastrophic values >10^6 (CH_4 + 0.1% TMAE)
R < 100 is still considered as moderate aging.

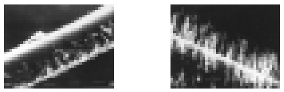

2 examples of deposits on anode wires

(Kadyk)

Aging can be minimized by

- **careful material selection and cleanliness during chamber construction**
- **chamber geometry and operation (wire diameter + material, gain)**
- **aging resistant gases: small admixture of**
  - **H_2O: increases surface conductivity)**
  - **alcohols, ether, methylal: good quenching capabilities, i.e. reduce lateral avalanche propagation + suppress polymerization**
- **clean gas systems, no PVC tubes, no soft rubber seals, no oil (bubblers), no fingerprints…**

Silicon detectors

Silicon detectors

Solid state detectors have a long tradition for energy measurements (Si, Ge, Ge(Li)).

Why do we use them as precision trackers?

Some characteristic numbers for silicon

Γ Band gap: E_g =1.12 V.

Γ E(e⁻-hole pair) = 3.6 eV, (≈ 30 eV for gas detectors).

Γ High specific density (2.33 g/cm³) → ΔE/track length for M.I.P.'s.: 390 eV/µm ≈ 108 e-h/ µm (average)

Γ High mobility: μ_e =1450 cm²/Vs, μ_h = 450 cm²/Vs

Γ Detector production by microelectronic techniques → small dimensions → fast charge collection (<10 ns).

Γ Rigidity of silicon allows thin self supporting structures. Typical thickness 300 µm → ≈ 3.2 ·10⁴ e-h (average)

H But: No charge multiplication mechanism!

Silicon detectors

How to obtain a signal ?

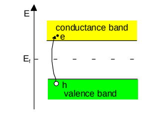

In a pure intrinsic (undoped) material the electron density n and hole density p are equal. $n = p = n_i$

For Silicon: $n_i = 1.45 \cdot 10^{10}$ cm^{-3}

In this volume we have $4.5 \cdot 10^8$ free charge carriers, but only $3.2 \cdot 10^4$ e-h pairs produced by a M.I.P.

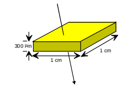

→ Reduce number of free charge carriers, i.e. deplete the detector

Most detectors make use of reverse biased p-n junctions

Silicon detectors

Spatial information by segmenting the p doped layer → single sided microstrip detector.

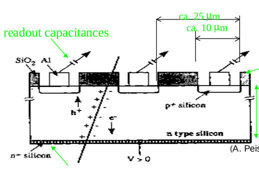

(A. Peisert, Instrumentation In High Energy Physics, World Scientific)

Highly n-doped layer defines end of depletion zone + good ohmic contact

A bit historical (mid 80's, when electronics was still bulky and expensive)
Reduced readout density: readout pitch < strip pitch

Capacitive charge sharing
Strip pitch 20 µm

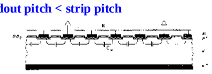

Readout pitch [µm]	60	120	240
Spatial resolutions [µm]	4.3	7.5	20

ACCMOR collaboration

Silicon Detectors

Segmenting also the n doped layer → Double sided microstrip detector.
But:

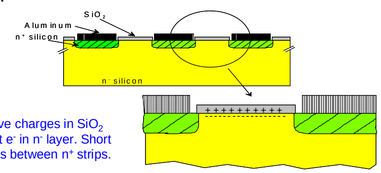

Positive charges in SiO_2 attract e⁻ in n⁻ layer. Short circuits between n⁺ strips.

Two solutions:

Add p⁺ doped blocking strips

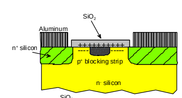

Add Aluminum layer on top of SiO_2
Negative biased MOS (metal oxide semiconductor) structure repelling e⁻

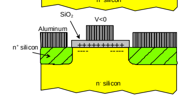

Silicon detectors

- **Silicon pixel detectors**
  - **Segment silicon to diode matrix**
  - **also readout electronic with same geometry**
  - **connection by bump bonding techniques**

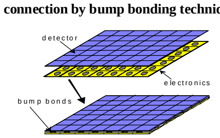

RD 19, E. Heijne et al., NIM A 384 (1994) 399

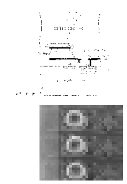

- **Requires sophisticated readout architecture**
- **First experiment WA94 (1991), WA97**
- **OMEGA 3 / LHC1 chip (2048 pixels, 50x500 µm²) (CERN ECP/96-03)**
- **Pixel detectors will be used in all future LHC experiments**

Silicon Detectors

- The DELPHI micro vertex detector (since 1996)

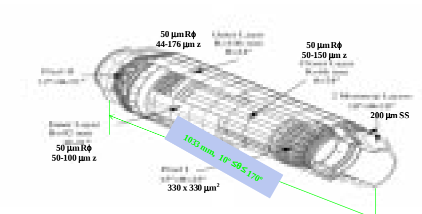

readout channels
ca. 174 k strips, 1.2 M pixels
total readout time: 1.6 ms

Total dissipated power 400 W
→ water cooling system

Hit resolution in barrel part
≈ 10 µm
Impact parameter
resolution (rϕ)

$$28\mu m \oplus 71/\left(p\sin^{\frac{3}{2}}\theta\right)$$

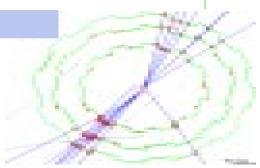

37

Silicon Detectors

- **Charge Coupled Devices (CCD)**

MOS structure with segmented metal layer

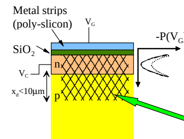

collect free electrons in a potential well, ca. 1µm below SiO_2 layer

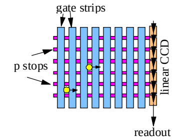

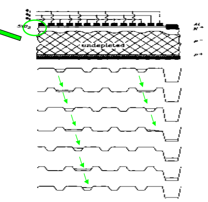

→ all pixels are readout via one (few) output node(s)
→ very few electronic channels but long readout time!

Charge transport by periodic change of gate voltage triplets (ϕ_1,ϕ_2,ϕ_3)

38

Silicon Detectors

Example: SLD VXD3 detector (since '96)

96 CCD's × 3.2·10⁶ = 3.07 ·10⁸ pixels (20 × 20 µm²)

Operation at T = -50°C

Each CCD is readout through 4 output nodes

Analogue information 8 bit FADC

total readout time = 200 ms (beams collide every 8.3 ms)

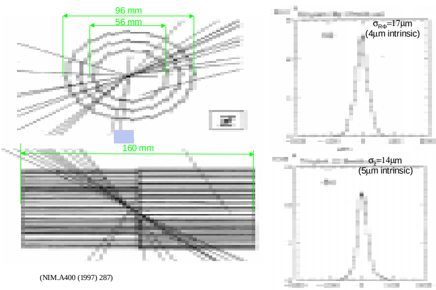

(NIM A400 (1997) 287)

39

Silicon Detectors

- **Silicon drift chamber**

(First proposed by E. Gatti and P. Rehak, NIM 255 (1984) 608)

principle:

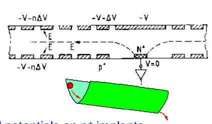

Define graded potentials on p⁺ implants
Measure arrival time at n⁺ strip

Segmentation of
n⁺ strip into pads
→ 2-D readout

CERES (NA45):
doublet of 3'' radial
Si drift chambers

Intrinsic resolution:
$\sigma_R \approx$ 20 µm, $\sigma_\phi \approx$ 2 mrad

U. Faschingbauer et al. NIM A 377 (1996) 362, W. Chen et al, IEEE NS-39 No. 4 (1992) 619

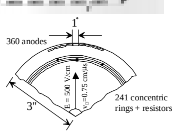

40

Scintillation

Scintillation

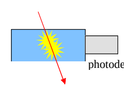

Energy deposition by ionizing particle
→ production of scintillation light (luminescense)

Scintillators are multi purpose detectors

- calorimetry
- time of flight measurement
- tracking detector (fibers)
- trigger counter
- veto counter
- .....

Two material types: Inorganic and organic scintillators

high light output
but slow

lower light output
but fast

41

Inorganic scintillators

Properties of some inorganic scintillators							
Table A6.2 properties of some inorganic scintillators							
Scintillator composition	Density (g/cm3)	Index of refraction	Wavelength of maximum emission (nm)	Decay time constant (us)	Scintillation pulse height1)	notes	Photons/MeV
NaI	3.67	1.78	303	0.06	190	2)	
NaI(T1)	3.67	1.85	410	0.25	100	3)	4.00E+04
CsI	4.51	1.8	310	0.01	6	3)	
CsI(T1)	4.51	1.8	565	1	45	3)	1.10E+04
CaI(Na)	4.51	1.84	420	0.63	85	3)	
KI(T1)	3.13	1.71	410	0.24/2.5	24	3)	
6LiI(Eu)	4.06	1.96	470-485	1.4	35	3)	1.40E+04
CaF2	3.19	1.44	435	0.9	50		
BaF2	4.88	1.49	190/220	0.0006	5		6.50E+03
			310	0.63	15		2.00E+03
Bi4Ge3O12	7.13	2.15	480	0.3	10		2.80E+03
CaWO4	6.12	1.92	430	0.5/20	50		
ZnWO4	7.87	2.2	480	5	26		
CdWO4	7.9	2.3	540	5	40		
CsF	4.65	1.48	390	0.005	5	3)	
CeF3	6.16	1.68	300	0.005	5		
			340	0.02			
ZnS(Ag)	4.09	2.35	450	0.2	150	4)	
GSO	6.71	1.9	440	0.06	20		
ZnO(Ga)	5.61	2.02	385	0.0004	40	4)	
YSO	4.45	1.8	420	0.035	50		
YAP	5.5	1.9	370	0.03	40		
PbWO4	8.28	1.82	440,530				100
LAr	1.4	1.295)	120-170	0.005/0.860			
LKr	2.41	1.405)	120-170	0.002/0.085			
LXe	3.06	1.605)	120-170	0.003/0.022			4.00E+04

1)relative to NaI(Tl) 2)at 80 K 3)hygroscopic 4)polycrystalline 5)at 170nm

42

Scintillator readout

ATLAS Hadron Calorimeter: (ATLAS) TDR

Scintillating tile readout via fibers and photomultipliers

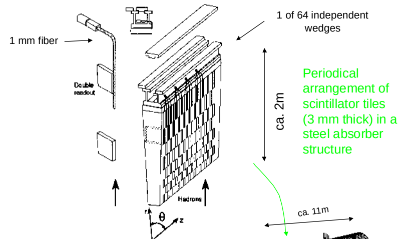

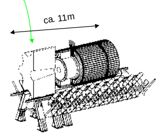

Each tile is read out on both outer sides

Photo detectors

- **Energy resolution of PM's**

The energy resolution is determined mainly by the fluctuation of the number of secondary electrons emitted from the dynodes.

Poisson distribution: $P(\bar{n},m)=\frac{\bar{n}^m e^{-m}}{m!}$

Relative fluctuation: $\frac{\sigma_n}{\bar{n}}=\frac{\sqrt{\bar{n}}}{\bar{n}}=\frac{1}{\sqrt{\bar{n}}}$

Fluctuations biggest, when $\bar{n}$ small ! → First dynode !

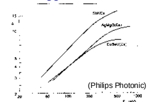

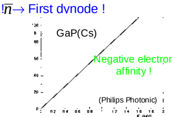

Illustration of a pulse height spectrum of a PM. First dynode: δ = 25

(Gilmore)

Photo Detectors

Dyn

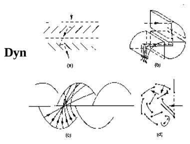

(Philips Photonics)

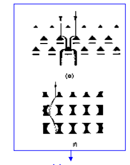

position sensitive PM's

Multi Anode PM
example: Hamamatsu R5900 series.

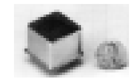

Up to 8x8 channels.
Size: 28x28 mm^2.
Active area 18x18 mm^2 (41%).
Bialkali PC: Q.E. = 20% at λ_{max} = 400 nm. Gain ≈ 10^6.

Gain uniformity and cross-talk used to be problematic, but recently much improved.

Photo Detectors

Micro Channel plates

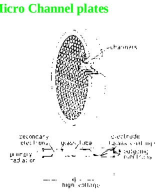

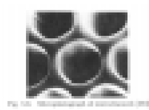

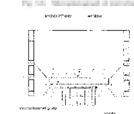

(Philips Photonics)

+ fast signal (transit time spread ≈ 50 ps),
+ less sensitive to B-field (0.1 T)
+ 2-dimensional readout possible
- limited life time (0.5 C/cm^2)
- limited rate capability (μA/cm^2)

Photo Detectors

- **Photo diodes**

P(I)N type

(sketches from J.P. Pansart, NIM A 387 (1997), 186)

High Q.E. (≈80% at λ ≈ 700nm), gain G = 1.

- **Photo triodes** = single stage PMT (no Silicon !)

G ≈ 10.
work in axial B-fields of 1T
OPAL, DELPHI: readout of lead glass in endcap calorimeter
G at 1T ≈ 7-10

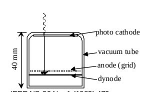

IEEE NS-30 No. 1 (1983) 479

- **Avalanche Photo diodes (APD)**

(J.P. Pansart, NIM A 387 (1997), 186)

High reverse bias voltage ≈ 100-200V.
High internal field → avalanche multiplication.
G ≈ 100

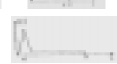

Photo Detectors

- **Visible Light Photo Counter VLPC**

Si:As impurity band conduction avalanche diode

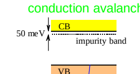

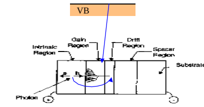

Hole drifts towards highly doped drift region and ionizes a donor atom → free electron. Multiplication by ionization of further neutral donor atoms.

M. Wayne, NIM A387 (1997) 278

Operation at low bias voltage (7V)
High IR sensitivity → Device requires cooling to LHe temperature.

Q.E. ≈ 60% around 500 nm.
Gain up to 15.000 !

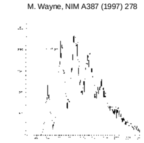

Successfully operated in Fermilab E835 fiber tracker.

Under test for D0 fiber tracker (72.000 fibers)

Photo Detectors

- **Hybrid photo diodes (HPD)**

  = photo cathode + p.e. acceleration + silicon det.
  (pixel, strip, pads)

proximity focusing
(i.e. no focussing)

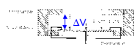

cross focusing

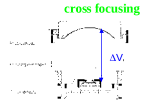

Photo cathode like in PMT, ΔV 10-20 kV

$$G = \frac{e\Delta V}{W_{Si}} = \frac{20\,keV}{3.6\,eV} \approx 5\cdot 10^3$$ (for ΔV =20 kV)

Single photon detection with high resolution

Poisson statistics with $\overline{n}$ =5000 !

Background from electron backscattering from silicon surface

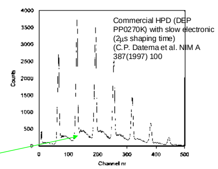

Photo Detectors

Imaging with HPD's

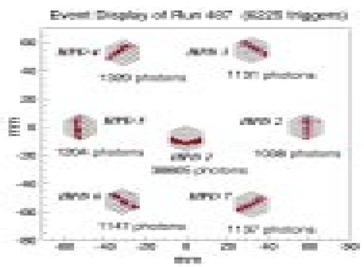

Commercial HPD's (DEP 61 hexagonal pixels) detect Cherenkov rings (C_4F_{10} and aerogel) in LHCb RICH prototype
(LHCB technical proposal)

Problem: active area fraction still too small !

Photo Detectors

Development of a 2048 pad HPD for RICH detectors
(LHC-b, CERN, Bologna, CdF)
Aim for active area > 80%.

(LHCb 98-007, RICH)

Fountain focusing. Demagnification ≈ 2.4

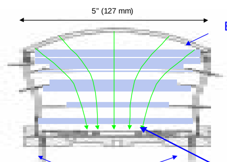

Bialkali photocathode

40 pins (vacuum feedthroughs)

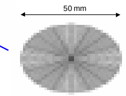

Silicon detector
16 x 128 = 2048 pads
(1x1 mm^2)
analogue electronics
(16 VA3 chips) inside tube

Scintillating fiber tracking

Scintillating fiber tracking

- Scintillating plastic fibers
- Capillary fibers, filled with liquid scintillator

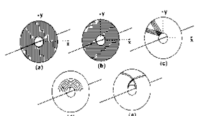

Planar geometries
(end cap)

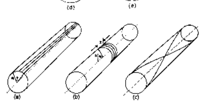

Circular geometries
(barrel)

a) axial
b) circumferential
c) helical

(R.C. Ruchti, Annu. Rev. Nucl. Sci. 1996, 46,281)

- High geometrical flexibility
- Fine granularity
- Low mass
- Fast response (ns) (if fast raed out) → first level trigger

Scintillating fiber tracking

Charged particle passing through a stack of scintillating fibers (diam. 1mm)

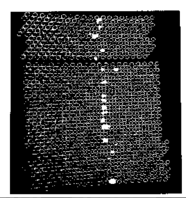

Hexagonal fibers with double cladding.

Only central fiber illuminated.

Low cross talk !

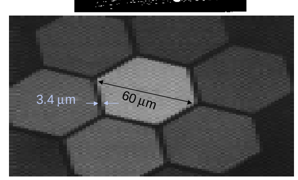

(H. Leutz, NIM A 364 (1995) 422)

Scintillating fiber tracking

CHORUS
scintillating fiber tracking

(PPE-97-033, PPE-97149)

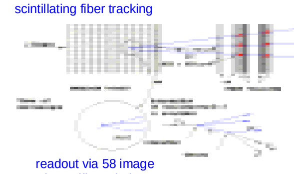

63.000 fibers
Ø0.5mm

readout via 58 image intensifiers chains

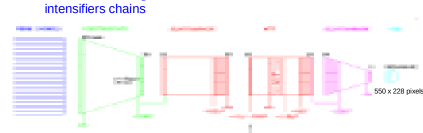

3 p.e. / mm fiber
σ = 140 μm
2 track resolution 500 μm

Particle Identification

■Particle Identification

■Particle identification is an important aspect of high energy physics experiments.

■Some physical quantities are only accessible with sophisticated particle identification (B-physics, CP violation, rare exclusive decays).

■One wants to discriminate: π/K, K/p, e/π, γ/π^0….

■The applicable methods depend strongly on the interesting energy domain. $\varepsilon_{xx} = N_x^{tag}/N_x$

■Depending on the physics case either ε_{xx} or ε_{xy} $\varepsilon_{xy} = N_y^{tag}/N_y$

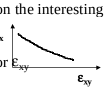

■has to be optimized: $R_{xy} = \varepsilon_{xx}/\varepsilon_{xy}$

■Efficiency:

■Misidentification: $D_{x,y} = \frac{Q_x - Q_y}{\sigma_Q}$

■Rejection:

dE/dx measurement

■ dE/dx in the DELPHI microvertex detector (4 layers)

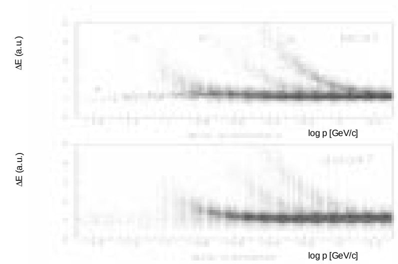

Time of flight

■Time of flight

$$\Delta t = \frac{L}{c}\left(\frac{1}{\beta_1} - \frac{1}{\beta_2}\right) = \frac{L}{c}\left(\sqrt{1 + m_1^2c^2/p^2} - \sqrt{1 + m_2^2c^2/p^2}\right) \approx \frac{Lc}{2p^2}\left(m_1^2 - m_2^2\right)$$

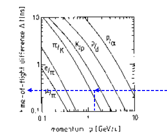

Δt for L = 1 m path length

Scintillator σ_t = 300 ps
π/K separation up to 1 GeV/c

Particle ID in ALICE: Option TOF with Pestov spark counters
π/K separation up to 2 GeV/c requires $\sigma_t \approx$ 100 ps (L=3m)

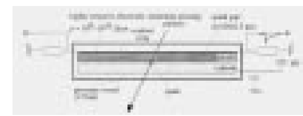

In test beam: $\sigma_t \approx$ 40 ps !

(ALICE technical proposal)

Cherenkov detectors

■Cherenkov radiation

■Cherenkov radiation is emitted when a charged particle passes a dielectric medium with velocity

$\beta > \beta_{thr} = \frac{1}{n}$ n: refractive index

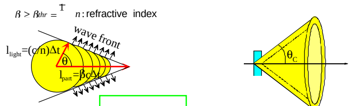

$\cos\theta_C = \frac{1}{n\beta}$ with $n = n(\lambda) \geq 1$

$\beta_{thr} = \frac{1}{n} \rightarrow \theta_C = 0$ threshold

$\theta_{max} = \arccos\frac{1}{n}$ 'saturated' angle (β=1)

Number of emitted photons per unit length and unit wavelength interval

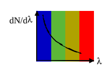

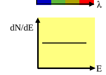

■ $\frac{d^2N}{dxd\lambda} = \frac{2\pi z^2\alpha}{\lambda^2}\left(1 - \frac{1}{\beta^2 n^2}\right) = \frac{2\pi z^2\alpha}{\lambda^2}\sin^2\theta_C$

$\frac{d^2N}{dxd\lambda} \propto \frac{1}{\lambda^2}$ with $\lambda = \frac{c}{\nu} = \frac{hc}{E}$ $\frac{d^2N}{dxdE} = const.$

Cherenkov detectors

■Particle ID with Cherenkov detectors

■ Detectors can exploit

$N_{ph}(\beta)$: threshold detector (do not measure θ_C)
$\theta(\beta)$: differential and
Ring Imaging Cherenkov detectors "RICH"

Threshold Cherenkov detectors

$N \propto 1 - \frac{1}{n^2\beta^2}$
$= 1 - \frac{1}{n^2}\left(1 + m^2/p^2\right)$

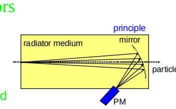

Example: study of an Aerogel threshold detector for the BarBar experiment at SLAC

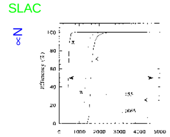

Two aerogel radiators
A1: n = 1.055
A2: n=1.0065
p > 0.4 GeV/c: π in A1
p > 1.2 GeV/c: π in A1 and A2
p > 1.4 GeV/c: K in A1
p > 4.2 GeV/c: K in A1 and A2
π/K separation between .4 and 4.2 GeV/c

Cherenkov detectors

■ Principle of operation of a RICH detectors

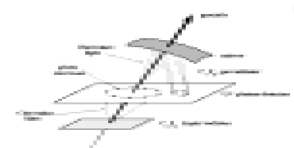

A RICH with two radiators to cover a large momentum range. π/K/p separation 0.7 - 45 GeV/c: DELPHI and SLD

Two particles from a hadronic jet (Z-decay) in the DELPHI gas and liquid radiator + hypothesis for π and K

(W. Adam et al. NIM A 371 (1996) 240)

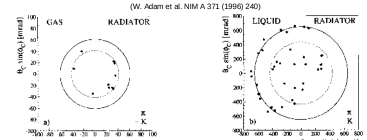

Cherenkov detectors

- Photo detectors for RICHes
- Photomultiplier (multi anode), Hybrid Photo Diodes
- Wire chambers
  - gaseous photocathodes
  - solid photocathodes
- Gaseous photocathodes
- Admix photosensitive agent to detector gas

molecule	formula	E_I [eV] (λ_I [nm])	max. ε_Q (E)	l_{ph} (at 293K)
TEA	$(C_2H_5)_3N$	7.5 (164)	0.33 (8.2)	0.43 mm
TMAE	$C_2[(CH_3)_2N]_4$	5.36 (230)	0.51 (8.3)	26 mm
DMA	$(CH_3)_2NH$	8.3 (148)	0.2 (9.2)	
TMA	$(CH_3)_3N$	7.9 (156)	0.27 (8.6)	

- Most running experiments use TMAE
- but: Low vapor pressure. TMAE (and the whole detector) need to be heated to reach a acceptable absorption length l_{ph}.
- Example DELPHI: $T_{TMAE} = 28°C \rightarrow l_{ph} \approx$ 16 mm
- Successful operation of TEA has been demonstrated.
- Short conversion length $\rightarrow$ 'fast' detectors
- DMA and TMA less attractive because of high thresholds E_I